A Theoretical Understanding of the Physical Mechanisms of Electrospinning

Chitral J. Angammana and Shesha H. Jayaram
High Voltage Engineering Lab (http://www.power.uwaterloo.ca/HVEL/)
Department of Electrical and Computer Engineering, University of Waterloo
200 University Ave., Waterloo, ON, N2L 3G1, Canada
phone: (1) 519-888-4567
e-mail: cjangamm@uwaterloo.ca, jayaram@uwaterloo.ca

***Abstract*— More recently, electrospinning models have been developed so that the electrospinning process could be approximately analyzed based on the parameters that govern the process. However, parametric analysis and accounting complex electrode geometries in the simulation are extremely difficult since the non-linearity nature in the problem. Therefore, the aim of the present work is to develop an existing electrospinning model for viscoelastic liquids in COMSOL Multiphysics for further analysis using the multi-physics analyzing capabilities in the software.**

I. INTRODUCTION

Electrospinning is a straightforward and inexpensive process that produces continuous nanofibres from submicron diameters down to nanometre diameters. The process involves an electrically charged jet of polymer solution or polymer melt consisting of polymer molecules with a chain sufficiently long that they do not break up due to Rayleigh instability. The basic principles for dealing with electrified fluids were published in a series of papers by Taylor in the early 1960s [1, 2]. His ideas later became known as the leaky dielectric model. With the advancement of nanotechnology and the popularity of the electrospinning process, several other mathematical models were developed in order to describe the behaviour of the electrospun jet. More recently, electrospinning models have been created so that the electrospinning process could be approximately analyzed based on the parameters that govern the process. As shown in Fig. 1, the electrospinning process consists of three stages that correspond to the behaviour of the electrospun jet: the formation of the Taylor cone, the ejection of the straight jet, and the unstable whipping jet region.

The surface of the fluid droplet that is held at the spinneret by its own surface tension becomes electrostatically charged with the application of high voltage. As shown in Fig. 1, the interactions of the electrical charges in the polymer solution with the external elec

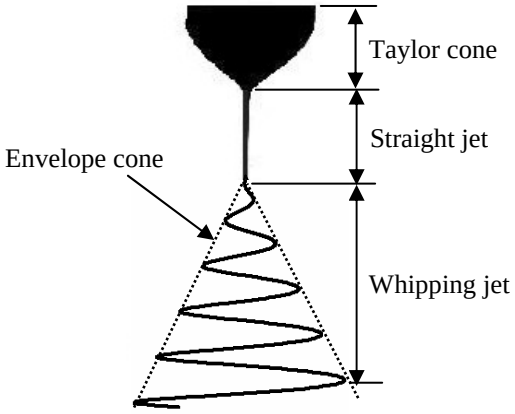

Fig. 1: Behaviour of the electrospun jet.

tric field result in the formation of the well-known Taylor cone [2]. In [1] and [3], a theoretical explanation has been given for the loss of stability and the formation of Taylor cone from electrified fluid droplets. When the Taylor cone is subjected to a very strong electric field with an appropriate field gradient at the tip of the cone, the droplet becomes unstable, and a single fluid jet is drawn out from the apex of the Taylor cone, as shown in Fig. 1. After traveling straight down for a specific position of its path, the ejected liquid jet usually becomes unstable with respect to the jet propagation. In a study conducted by Hohman et al., they developed a theoretical framework for understanding the physical mechanisms of electrospinning and proposed a method of quantitatively predicting the parameter regimes where the electrospinning occurs [4]. Feng et al. simplified the Hohman's model by eliminating the ballooning instability of the electric field calculation. The simplified model was tested by comparing its predictions with the experimental data for a variety of boundary conditions and parameter values, such as the electric Peclet number, the Froude number, the Reynolds number, and the Weber number. Non-Newtonian rheology was also introduced into the theoretical model of electrospinning, and the effects of extension thinning, extension thickening, and strain hardening of the polymer solution were examined [5]. Reneker et al. and Yarin et al. contributed significantly to the modeling of electrospinning by developing a discrete three-dimensional model to describe the dynamics of electrospinning [6, 7].

The aim of the present work is to further analyze the electrospinning process based on an existing electrospinning model for viscoelastic liquids using a finite element method software named COMSOL® Multiphysics.

II. Model development

Once the jet flows away from the Taylor cone in a nearly straight line, the travelling liquid jet is subjected to a variety of forces, such as a Coulomb force, an electric force imposed by the external electric field, a viscoelastic force, a surface tension force, a gravitational force, and an air drag force [6]. Therefore, the electrospun jet can be represented by four steady-state equations as follows [4, 5]. The notations are provided in Table I.

TABLE I : SYMBOLS EMPLOYED AND THEIR DEFINITIONS.

Symbol	Definition	Units
R	Jet radius	m
Q	Volume flow rate	m^3/s
E	z component of the electric field	V/m
v	Velocity of the jet	m/s
K	Conductivity of the solution	S/m
σ	Surface charge density	C/m^2
I	Jet current	A
ρ	Fluid density	Kg/m^3
τ_{zz}	Viscous normal stress in the axial direction	N/m^2
p	Pressure	N/m^2
γ	Surface tension of the solution	N/m
t_t^e	Tangential stress exerted on the jet surface due to the electric field	N/m^2
t_n^e	Normal stress exerted on the jet surface due to the electric field	N/m^2
E_∞	External electric field	V/m
τ_{prr}	Radial polymer normal stress	N/m^2
τ_{pzz}	Axial polymer normal stress	N/m^2
λ	Relaxation time	s
η_p	Viscosity of the solution due to the polymer	Pas
η_0	Viscosity of the solution at zero shear rate	Pas
α	Mobility factor	-
ε_{air}	Dielectric constant of the ambient air	-
ε	Dielectric constant of the solution	-
R_0	Jet radius at the origin	m

1. Conservation of mass

$$\frac{d\left(\pi R^2 v\right)}{dz} = 0 \tag{1}$$

2. Conservation of charge

$$\frac{d}{dz}\left(2\pi R\sigma v + \pi R^2 KE\right) = 0 \tag{2}$$

3. Conservation of momentum

$$\frac{d\left(\pi R^2 \rho v^2\right)}{dz} = \pi R^2 \rho g + \frac{d}{dz}\left(\pi R^2\left(-P + \tau_{zz}\right)\right) + \frac{\gamma}{R}\left(2\pi R\left(\frac{dR}{dz}\right)\right) + 2\pi R\left(t_t^e - t_n^e\left(\frac{dR}{dz}\right)\right) \tag{3}$$

4. Coulomb's integral for the tangential electric field inside the jet

$$E - \ln\frac{1}{\chi}\left[\frac{\beta}{2}\frac{d^2\left(R^2E\right)}{dz^2} - \frac{1}{\varepsilon_{air}}\frac{d\left(\sigma R\right)}{dz}\right] = E_\infty \tag{4}$$

In addition, Equations (5) and (6) are considered here to represent the non-uniform uni-axial extension of viscoelastic polymer solutions [8].

$$\tau_{prr} + \lambda\left(v\tau'_{prr} + v'\tau_{prr}\right) + \alpha\frac{\lambda}{\eta_p}\tau_{prr}^2 = -\eta_p v' \tag{5}$$

$$\tau_{pzz} + \lambda\left(v\tau'_{pzz} - v'\tau_{pzz}\right) + \alpha\frac{\lambda}{\eta_p}\tau_{pzz}^2 = 2\eta_p v' \tag{6}$$

The Equations (1) to (6) can be transformed into dimensionless form using the dimensionless parameters and groups that are shown in Table II and Table III.

TABLE II: CHARACTERISTICS PARAMETERS EMPLOYED AND THEIR DEFINITIONS.

Parameters	definition
Length	R_0
Velocity	$v_0 = \frac{Q}{\pi R_0^2}$
Electric field	$E_0 = \frac{I}{\pi R_0^2 K}$
Surface charge density	$\sigma_0 = \varepsilon_{air} E_0$
Viscous stress	$\tau_0 = \frac{\eta_0 v_0}{R_0}$

Inserting these dimensionless parameters and groups into the equations (1) to (6) gives the following dimensionless equations.

$$R^2 v = 1 \tag{7}$$

$$ER^2 + PeRv\sigma = 1 \tag{8}$$

$$v\frac{dv}{dz} = \frac{1}{Fr} + \frac{3\left(1-r_n\right)}{\mathrm{Re}\,R^2}\frac{d}{dz}\left(R^2\frac{dv}{dz}\right) + \frac{1}{\mathrm{Re}}\frac{T'_P}{R^2} + \frac{1}{WeR^2}\frac{dR}{dz} + E_p\left(\sigma\frac{d\sigma}{dz} + \beta E\frac{dE}{dz} + \frac{2E\sigma}{R}\right) \tag{9}$$

$$E - \ln\chi\left[\frac{\beta}{2}\frac{d^2\left(ER^2\right)}{dz^2} - \frac{d\left(\sigma R\right)}{dz}\right] = E_\infty \tag{10}$$

$$\tau_{prr} + De\left(v\tau'_{prr} + v'\tau_{prr}\right) + \alpha\frac{De}{r_\eta}\tau_{prr}^2 = -r_\eta v' \tag{11}$$

$$\tau_{pzz} + De\left(v\tau'_{pzz} - v'\tau_{pzz}\right) + \alpha\frac{De}{r_\eta}\tau_{pzz}^2 = 2r_\eta v' \tag{12}$$

TABLE III: DIMENSIONLESS GROUPS EMPLOYED AND THEIR DEFINITIONS.

Group	definition	Group	definition
Froude number	$Fr = \frac{v_0^2}{gR_0}$	Aspect ratio	$\chi = \frac{L}{R_0}$
Reynolds number	$\mathrm{Re} = \frac{\rho v_0 R_0}{\eta_0}$	Peclet number	$Pe = \frac{2\varepsilon_{air} v_0}{KR_0}$
Weber number	$We = \frac{\rho v_0^2 R_0}{\gamma}$	Electrostatic force parameter	$E_p = \frac{\varepsilon_{air} E_0^2}{\rho v_0^2}$
Deborah number	$De = \frac{\lambda v_0}{R_0}$	Ratio of dielectric constant	$\beta = \frac{\varepsilon}{\varepsilon_{air}} - 1$
Viscosity ratio	$r_\eta = \frac{\eta_p}{\eta_0}$	Tensile force	$T_P = R^2\left(\tau_{pzz} - \tau_{prr}\right)$

As shown in Fig. 2, the boundary conditions are applied at $z = 0$ and $z = \chi$. Equations (13), (14), (15), and (16) represent the boundary conditions at $z = 0$. Similarly, Equations (17) and (18) give the boundary conditions at $z = \chi$.

$$R(0) = 1 \tag{13}$$

$$E(0) = E_0 \tag{14}$$

$$\tau_{prr}(0) = 2r_\eta \frac{1}{R^3}\frac{dR}{dz} \tag{15}$$

$$\tau_{pzz}(0) = -2\tau_{prr} \tag{16}$$

$$E(L) = E_\chi \tag{17}$$

$$R(L) + 4z\frac{dR(L)}{dz} = 0 \tag{18}$$

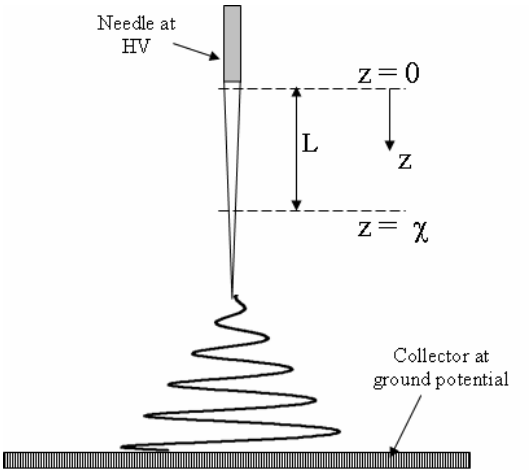

Fig. 2: Illustration of boundary conditions.

The above mathematical model is formulated using the partial differential equation (PDE) module in the software named COMSOL Multiphysics. In addition, the results of a parametric study investigating the effects of the solution conductivity and the magnitude of the external electric field on fibre diameter are presented in the following section.

III. RESULTS

A solution is obtained through the model using the desired material parameters of $\mathrm{Re} = 2.5\times10^{-3}$, $We = 0.1$, $Fr = 0.1$, $Pe = 0.1$, $E_p = 1$, $\beta = 40$, $\chi = 5$, and $De = 10$. The results match quite well with the previous works that have been published in [5, 8]. As shown in Fig. 3 (a), the rate of thinning of *R* is maximum at *z = 0*, and then it relaxes smoothly with the growth of the jet. On the other hand, *E* shoots up to a peak value and then relaxes over the progression of the jet. The electric field *E* is mainly induced by the axial gradients of surface charges $\left(d(\sigma R)/dz\right)$ [5]. For the parameters considered, it can be estimated as $\left(d(\sigma R)/dz\right) \approx -\left(2R\,dR/dz\right)/Pe$. Therefore, Equation (10) becomes $\left(dE/dz\right) \approx \ln\chi\left(d^2R^2/dz^2\right)/Pe$, which is a large positive number, hence *E* initially shoots up [5]. Physically, the amount of charges that can be conducted reduces with decreasing jet radius. However, to maintain the same jet current, the convection has to carry more surface charges. Therefore, the density of surface charge gradually increases in the region that has been considered in the simulation (χ<5). As the jet gets thinner and

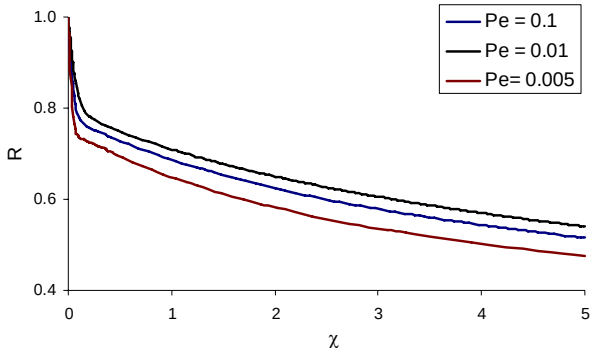

(a)

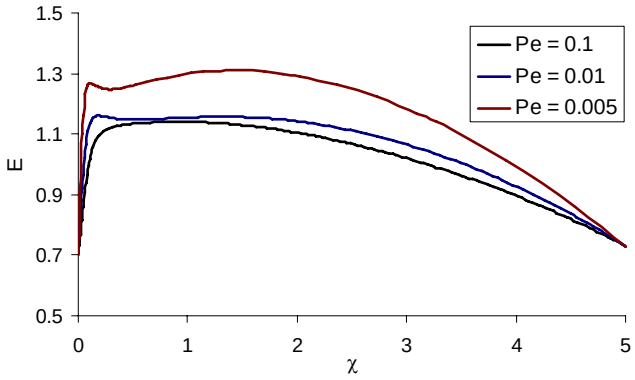

(b)

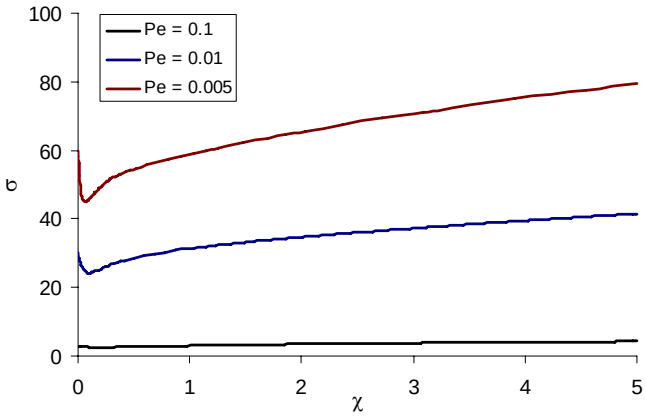

(c)

Fig. 3: Solutions for (a) R; (b) E; and (c) σ for varying values of Pe.

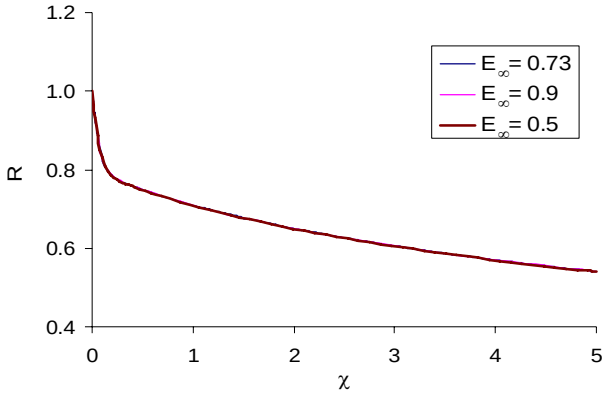

(a)

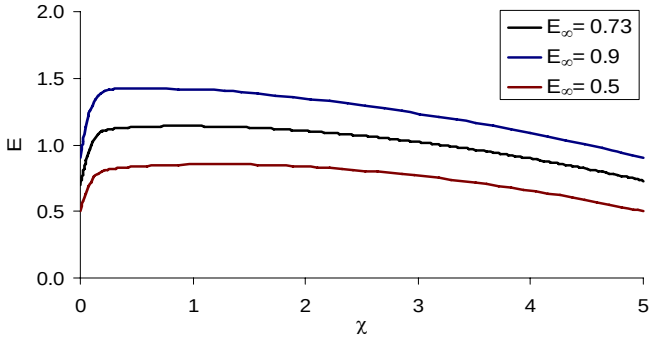

(b)

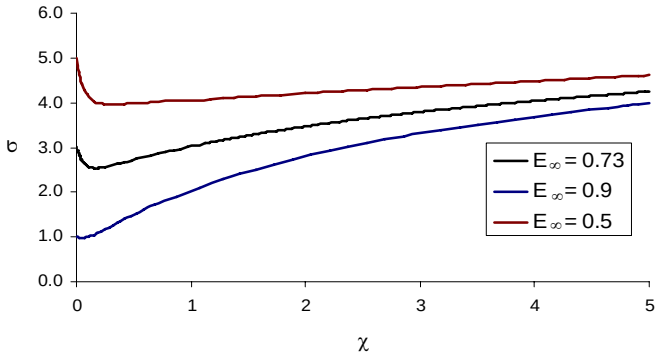

(c)

Fig. 4: Solutions for (a) R; (b) E; and (c) σ for varying values of E_∞.

faster, electric conduction gradually transfers to convection [5]. The initial oscillation that is observed in σ appears due to the chosen value of $\sigma(0)$. This has been discussed in [5] in more detail. Fig. 3 (a), (b), and (c) show the variation of dimensionless radius of the jet (R), the total electric field (E), and the surface charge density (σ) for different Pe values which is directly proportional to the conductivity K of the solution. As shown in Figures 3 (a) and (c), increasing Pe decreases the stretching of the jet as a result of weaker electrostatic pulling force with the decrease of the surface charge density at the fluid surface.

As shown in Fig. 4 (a) and (b), the external electric field E_∞ is insensitive to the thinning of the electrospun jet. The reason is the decrease of electrostatic pulling force in consequence of the reduction of surface charge density (as shown in Fig. 4 (c)), if the current I is held at a constant value. However, in reality, the increase of the strength of the electric field also increases the jet current I, relatively linearly [4, 5]. Therefore, as reported in [5], E_p is a better parameter to reflect the variation of electric field than E_∞.

IV. Conclusions

An electrospinning model was formulated with the help of a finite element method software using an existing viscoelastic electrospinning model. The model was validated comparing the results that have been published by previous researchers. The model can be used for the advanced analysis such as complex electrode geometries using the multiphysics capabilities in COMSOL multyphysics.

References

[1] G. Taylor, "Disintegration of Water Drops in an Electric Field," *Proceedings of the Royal Society of London, Series A, Mathematical and Physical Sciences*, vol. 280, No. 1382, pp. 383-397, Jul. 1964.

[2] G. Taylor, "Electrically Driven Jets," *Proceedings of the Royal Society of London, Series A, Mathematical and Physical Sciences*, vol. 313, No. 1515, pp. 453-475, Dec. 1969.

[3] J. Zeleny, "Physical review," *Phy. Rev.*, vol. III, No. 2, pp. 69-91, Feb. 1914.

[4] M.M. Hohman, M. Shin, G. Rutledge, and M.P. Brenner, "Electrospinning and electrically forced jets. I. Stability theory," *Physics of Fluids*, vol. 13, No. 8, pp. 2201-2220, Aug. 2001.

[5] J.J. Feng, "The stretching of an electrified non-Newtonian jet: A model for electrospinning," *Physics of Fluids*, vol. 14, No. 11, pp. 3912-3926, Nov. 2002.

[6] D.H. Reneker, A.L. Yarin, H. Fong, and S. Koombhongse, "Bending instability of electrically charged liquid jets of polymer solutions in electrospinning," *J. Appl. Phys.*, vol. 87, 4531–4547, 2000.

[7] A.L. Yarin, S. Koombhongse, and D.H. Renekera, "Bending instability in electrospinning of nanofibers," *Journal of Applied Phy.*, vol. 89, No. 5, pp. 3018-3026, Mar. 2001.

[8] P.C. Roozemond, Report No. MT07.12, "A model for electrospinning viscoelastic fluids," Department of mechanical engineering, Eindhoven University of Technology, Netherlands, 2007.